ELSEVIER

Chemical Engineering Journal 138 (2008) 538–547

Chemical Engineering Journal

www.elsevier.com/locate/cej

Electrochemical promotion of bulk lattice-oxygen extraction for direct methane conversion to syngas in SOFCs with Ni-YSZ anodes

Ta-Jen Huang *, Meng-Chin Huang

Department of Chemical Engineering, National Tsing Hua University, Hsinchu 300, Taiwan, ROC

Received 9 May 2007; received in revised form 10 July 2007; accepted 11 July 2007

Abstract

A phenomenon of electrochemical promotion of lattice-oxygen extraction from the bulk phase of YSZ is observed during direct methane oxidation to generate syngas at 800 °C in solid oxide fuel cells (SOFCs) with Ni-YSZ (yttria-stabilized zirconia) anodes. Markedly higher amount of oxygen than that equivalent to the measured current is extracted for anodic oxidation. This promotion effect increases as the potential (voltage) increases. A phenomenon of "fuel-free current" is observed to be a consequence of this effect. The electrochemically promoted extraction of bulk lattice oxygen is influenced by both the operating condition and the reaction type. Both rate enhancement ratios of CO and CO_2 formations are linearly related to the measured current density but inversely linearly related to the voltage. As the current density increases, both methane conversion and CO selectivity increase. Electrochemical promotion of bulk lattice-oxygen extraction enhances the syngas generation.

Keywords: Electrochemical promotion; Bulk lattice-oxygen extraction; Fuel-free current; Methane oxidation; Syngas generation; Solid oxide fuel cell

1. Introduction

Electrochemical promotion or non-Faradaic electrochemical modification of catalytic activity (NEMCA) effect has been studied extensively [1–13]. This effect is due to electrochemically controlled migration of ionic species from the solid electrolyte onto the gas-exposed electrode surface. Upon application of an external potential, the migration of ionic species onto the gas-exposed catalyst-electrode surface causes a change in catalyst work function [5], which corresponds to a change in activation energy so as to affect the catalytic rate. In general, with increasing catalyst-electrode potential, the oxidation rate increases for electrophobic behavior and decreases for electrophilic behavior [6].

The Faradaic efficiency, Λ, for electrochemical promotion with O^{2-}-conducting supports is defined as

$$\Lambda = \frac{\Delta r}{(I/2F)} \tag{1}$$

where Δr is the current- or potential-induced change in catalytic rate, I is the applied current and F is Faraday's constant [10]. It is pointed out that only a fraction $(1/\Lambda)$ of the oxygen species from the support will be found in the reaction products [14]. This fraction becomes significant only at elevated temperature, i.e. $T > 550$ °C, where Λ approaches unity and the phenomenon of electrochemical promotion disappears. In other words, when a positive (anodic) current I is applied, O^{2-} is supplied to the catalyst at a rate $I/2F$; this support-supplied lattice oxygen species can act as a reactant but the reaction rate due to this oxygen is limited by $I/2F$ [9], i.e. limited by the current. It is also pointed out that two distinct types of oxygen present on supported metal surfaces, one promoting, the other highly active, are needed to complete the picture of the phenomenon for electrochemical promotion; consequently, the concept of the sacrificial promoter is essential for the interpretation of the effect of electrochemical promotion [14].

Methane decomposition over the Ni cermet anode is a major reaction for direct-methane solid oxide fuel cell (SOFC) [15,16]. Since methane decomposition over the Ni cermet anodes generally causes carbon deposition (coking) [17], self de-coking should be an important reaction. Notably, "self de-coking" means the removal of the produced or deposited carbon-containing species by the oxygen species from under the surface, the bulk-lattice oxygen, when there is no oxygen in the gas phase [18]. In the case of direct methane SOFC, self de-coking can be done by the oxygen species transported from the cathode

* Corresponding author. Tel.: +886 3 5716260; fax: +886 3 5715408.
E-mail address: tjhuang@che.nthu.edu.tw (T.-J. Huang).

1385-8947/$ – see front matter © 2007 Elsevier B.V. All rights reserved.
doi:10.1016/j.cej.2007.07.057

three-phase boundary (TPB) to the anode surface via the bulk of the oxygen-ion conducting materials. Therefore, an electrical current is generated during self de-coking in direct-methane SOFC.

During methane decomposition and self de-coking, the formation of only CO but not CO_2 should lead to a large difference in SOFC performance. This is because the electrochemical formation of CO_2 involves four electrons while that of CO involves only two electrons, with each oxygen ion carrying two electrons. Hence, the current density in CO_2 formation is twice that in CO formation. However, if the direct methane SOFC is used for the cogeneration of synthesis gas (syngas), i.e. $CO + H_2$, the formation of only CO but not CO_2 should help the selectivity for syngas. As for SOFC with the deposited carbon as fuel [19], the formation of only CO but not CO_2 would result in a much lower power generation.

Over gadolinia-doped ceria (GDC), a mixed ionic-electronic conductor, a new phenomenon of electrochemical promotion of lattice-oxygen extraction from GDC bulk is observed during direct methane oxidation, in the absence of anode-side gas-phase oxygen, to generate syngas at 800 °C [20]. However, no open-circuit measurements were carried out and thus some theories of traditional electrochemical promotion can not be applied to this new phenomenon of "electrochemical promotion of bulk lattice-oxygen extraction". Additionally, the electronic conductivity of GDC seems to help the occurrence of this new phenomenon [20]. Since the currently used electrolyte is frequently yttria-stabilized zirconia (YSZ), which is a pure oxygen-ion conductor, the study with YSZ would be desirable to expand the field of this new phenomenon. On the other hand, this new phenomenon of electrochemical promotion leads to a new phenomenon of "fuel-free current", whose application has been reported with Ni-YSZ anodes [21]. This gives some significance in the study of "electrochemical promotion of bulk lattice-oxygen extraction" with Ni-YSZ anodes.

In this work, a phenomenon of electrochemical promotion of bulk lattice-oxygen extraction from the anode-side YSZ materials is observed on methane oxidation over Ni-YSZ anode in an SOFC operating at 800 °C without oxygen in the anode-side gas phase. Markedly higher amount of oxygen than that equivalent to the measured current is extracted for anodic oxidation. The oxygen species from the anode bulk lattice are highly active and both rates of CO and CO_2 formations are substantially enhanced. This is a case that the concept of the sacrificial promoter is not applicable. Thus, there should be a difference in electrochemical promotion between the case with oxygen in the anode-side gas phase and the case without it. It is also found that the electrochemical promotion effect on CO formation can be much higher than that on CO_2 formation. This is beneficial for syngas generation in direct-methane SOFC.

2. Experimental

2.1. Preparation of Ni-YSZ powder

The Ni-YSZ powder for the anode is prepared by impregnating the YSZ (8 mol% yttria) powder (1.68 μm) with an aqueous solution of nickel nitrate (98% purity) in a ratio to make 60 wt% Ni with respect to YSZ. The mixture is heated with stirring to remove excess water and then place in a vacuum oven to dry overnight. The dried Ni-YSZ powder is heated to 900 °C and then cooled down to room temperature. After milling, the Ni-YSZ powder with Ni:YSZ = 3:5 in weight was obtained.

2.2. Construction of SOFC unit cell

The commercial YSZ tape (156 μm thickness, Jiuhow, Taiwan) was employed to make an electrolyte-supported cell. A disk of 1.25 cm diameter was cut from the tape. One side of the disk was coated with the Ni-YSZ paste, which was made of the above Ni-YSZ powder, coin oil, polyvinyl butyral, and ethanol. The other side of the disk was screen-printed with a thin layer of Pt paste (C3605P, Heraeus) to make the cathode layer.

The coating of the Ni-YSZ paste to make the anode layer was carried out by spinning coating with 2000 rpm for 9 times. Then, the both side-coated unit cell was heated in an oven, with a heating rate of 5 °C/min, to 300 °C, held for 2 h, then to 500 °C, held for 2 h, and then to 1400 °C, held for 2 h. The thus-prepared unit cell has an anode area of 1 cm^2, an anode thickness of about 30 μm, an electrolyte thickness of 156 μm, a cathode area of 1 cm^2, and a cathode thickness of about 5 μm. These thicknesses were measured from a scanning electron micrograph plot of the cross section of the unit cell.

Both sides of the completed unit cell were closely connected with gold mesh wires (100 mesh) for current collection, and then with Pt wires to the current and voltage measurement units. The ceramic paste was used to seal the unit cell in a quartz tube with a heat treatment of 400 °C for 1.5 h so as to complete the preparation of the test unit with a single cell. The anode side of the unit cell is sealed in the quartz tube and the cathode side is exposed to stagnant air.

2.3. Activity test of direct methane conversion

An external circuit resistance of 1 Ω, which is the lowest adjustable resistance of the load circuit in this work, was employed for some operations. For others, the external circuit resistance is varied, as described in the results. The test temperature is 800 °C throughout this work. The feed was 10% CH_4 in argon. The flow rate was always 100 ml/min passing the anode side.

The test started with anode reduction at 400 °C in 10% H_2 for 2 h. Then, argon flow was passed for 2 h to purge the system. The test unit was then heated in argon to 800 °C at a rate of 5 °C/min. Then, 10% H_2 was introduced for 30 min and argon flow was followed until the measured electrical current became zero. Test of direct-methane oxidation was then carried out with introducing CH_4 flow for a designated time. The details of the test procedure have been reported elsewhere [20].

A new test started with the above-described introduction of 10% H_2 for 30 min at 800 °C and with following argon flow until the measured electrical current became zero. However, if this H_2 test result showed a deactivation of the used unit cell, a

fresh unit cell would be used and the new test started with the above-described anode reduction at 400 °C.

Through out the test, electrical current, voltage, and outlet gas compositions were always measured. The compositions of CO and CO_2 were measured by CO-NDIR and CO_2-NDIR (non-dispersive infrared analyzer, Beckman 880), respectively. Other gas compositions were measured by two gas chromatographs (China Chromatography 8900) in series.

3. Results

3.1. Direct methane conversion to syngas

Fig. 1(a) indicates that a synthesis gas (syngas), consisting of H_2 and CO, can be produced via direct methane conversion over Ni-YSZ anode. Since there is no oxygen in the anode-side gas phase, the oxygen species for the partial oxidation of methane are considered to come from the cathode-side gas phase via the electrolyte. However, Fig. 2 reveals that the oxygen amount consumed for the formation of CO and CO_2, as represented by the equivalent current, can be much higher than that from the cathode-side gas phase, as represented by the measured current. Notably, zone I denotes the area between the curves of equivalent current and measured current and extends from time zero until these two curves meet; zone II denotes the area under the curve of measured current and to the right of the curve of equivalent current. Thus, additional amount of lattice oxygen is extracted, shown as zone I; these lattice oxygen species should come from the anode-side bulk. Notably, also, a measured current can occur only when the oxygen species, with each carrying two electrons, come from the cathode TPB and go to the anode TPB via the electrolyte; the oxygen species extracted only from the anode-side bulk lattice would not contribute to the measured current. In Fig. 2, the oxygen amount for the production of CO_x, i.e. CO and CO_2, is indicated by the equivalent current and also revealed by the oxygen-transfer rate. Notably, also, the current density and the oxygen-transfer rate, the left and right ordinate of Fig. 2, is related by 1 mA/cm^2 to 0.31088 μmol O^{2-}/cm^2 min. In other words, the oxygen species for partial oxidation of methane can come from either the cathode-side gas phase or the anode-side bulk lattice. Since NiO can be completely reduced to Ni at 400 °C [22], the oxygen species from the anode-side bulk lattice should come from only YSZ in this work, since the NiO-YSZ anode is reduced at 400 °C and then at 800 °C.

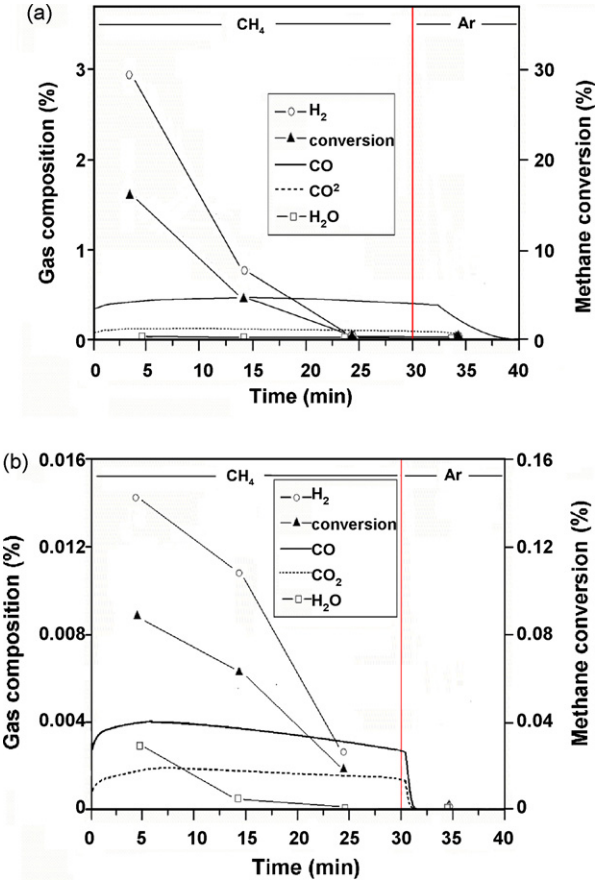

Fig. 1. Outlet gas composition and methane conversion during 30 min CH_4 flow. (a) Close circuit, 1 Ω circuit resistance and (b) open circuit.

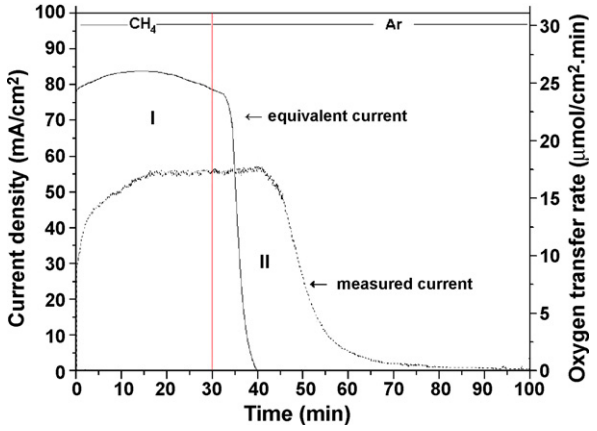

Fig. 2. Profiles of current densities vs. time. 30 min CH_4 flow; 1 Ω circuit resistance. Zone I denotes the area between the curves of equivalent current and measured current and extends from time zero until these two curves meet. Zone II denotes the area under the curve of measured current and to the right of the curve of equivalent current.

The "equivalent current" indicates the current which would be produced if the O species for CO_x formations at the anode TPB come from the cathode TPB. This CO_x equivalent current is calculated with the total amount of the O species in forming CO and CO_2, with each O species carrying two electrons, that is [(CO formation amount) + (CO_2 formation amount) × 2]/0.31088. Notably, the equivalent current in this work is equivalent to the formation rate of CO_x only; it should be equivalent to the total rate of formation of all the oxidation products. Therefore, the formation rate of other detectable oxidation products, only H_2O in this work, is included to calculate the total amount of lattice oxygen extracted for oxidation. Nevertheless, the amount of H_2O formed from CH_4 reactions was quite small during all the experiments of this work, for example, shown in Fig. 1(a). Keeping this in mind, although H_2O formation was measured by GC whose accuracy is less than that of CO_x measured by NDIR, the total amount of lattice oxygen extracted can be calculated with sufficient accuracy.

A comparison of Fig. 1(a) with (b) indicates that methane conversion, as indicated by the "conversion" curve, and the rates of CO and CO_2 formations can be markedly promoted with a flow of electrical current, under the condition of close circuit, relative to that without it, under open circuit. This is a phenomenon of electrochemical promotion since additional amount of lattice oxygen is extracted for CO_x formation, that is, the amount of oxygen for anodic oxidation is markedly higher than that of the measured current via the electrolyte. Notably, the term of "electrochemical promotion" is used here to follow the literature usage of this term to mean a promotion effect due to electrochemically controlled migration of ionic species from the solid electrolyte onto the gas-exposed electrode surface [1–13,20]. This electrochemically promoted CO_x formation is due to the promoted lattice-oxygen extraction from the anode-side bulk lattice [20]. The total amount of additionally extracted lattice oxygen for CO_x formation is indicated by zone I, in Fig. 2 for example. Notably, also, SOFC under open-circuit condition works as a conventional catalytic reactor; the catalytic oxidation as observed in Fig. 1(b) is due to the extraction of bulk lattice oxygen in the absence of gaseous oxygen [23–25].

Fig. 2 reveals a region, designated as zone II, for the generation of electrical current in the absence of any fuel, either in the gas phase or over the anode surface, the latter being the deposited carbon species from methane decomposition. Fig. 1(a) reveals the evidence for the absence of any fuel in relation to the occurrence of zone II, that is, both CH_4 conversion and H_2 concentration become zero well before switching to Ar flow. Separate GC measurements indicate that CH_4 concentration in the anode-side gas phase becomes zero in less than 2 min after switching to Ar flow, which means a very quick purge with high rate of Ar flow. Additionally, there is no any fuel-oxidation product, CO, CO_2 or H_2O as detectable in this work, associated with the occurrence of zone II. Therefore, the measured electrical current indicated by zone II is indeed a current generated in the absence of any fuel and can be termed a "fuel-free current" [21]. The occurrence of the fuel-free current is a consequence of the electrochemical promotion of lattice oxygen extraction from the anode-side bulk during the oxidation of the fuel, as will be clarified in Section 4.

In this work, the "fuel" means both methane and the deposited carbon species from methane decomposition. Fig. 1(a) presents the evidence for the existence of the deposited carbon species, that is, the amounts of CO and CO_2 formations exceed that allowed by methane converted, as indicated by the "conversion" curve, after about 15 min of CH_4 flow. The exceeding amounts of CO and CO_2 formations should be due to the oxidation of the deposited carbon species. These carbon species are usually considered to be surface CH_x ($x = 0$–3) species, which are intermediates of CH_4 decomposition over Ni [26]. On the other hand, before about 15 min CH_4 flow, the amount of CO_x formations are lower or much lower than that associated with methane conversion, indicating the occurrence of some methane decomposition without oxidation, which produces the deposited carbon species. However, since the amount of H_2O formation after about 25 min CH_4 flow becomes zero, the CH_x species should be mostly the C species, which may cause coking to deactivate the anode. Separate tests indicate that anode deactivation did not occur with 5 min methane flow, but did with 10 min or longer methane flow. Thus, CH_4 flow of only 5 min is employed for the following measurements to avoid the effect of anode deactivation.

3.2. Operation with varying circuit resistance

Table 1 indicates that the voltage increases and the current density decreases as the external circuit resistance increases. Notably, a decrease of the current density means a decrease of the transfer rate of the oxygen ion, i.e. the electron carrier, in the bulk of the oxygen-ion conducting YSZ materials. Fig. 3(A)–(E) presents the results of the variations of current density with time under different circuit resistance. The phenomenon of electrochemical promotion of bulk lattice-oxygen extraction, indicated by zone I, and that of fuel-free current, indicated by zone II, occurs in all cases. Notably, also, the profile of the equivalent current indicates the CO_x formation. From case A to case E, with decreasing current density, the lattice O species which can be additionally extracted from the anode-side bulk decreases, as also presented in Table 1. Consequently, the profile of the fuel-free current, the zone II profile, shows a flatter and longer tail, indicating a lower mobility of the lattice O species. Notably, the total O content in YSZ of the NiO-YSZ anode is 104.5 μmol; thus, the amount of additionally extracted lattice O species is significant, as shown in Table 1. It is possible that some lattice O species in YSZ of the electrolyte layer, which has a total O content of 2064 μmol, has been extracted.

Table 1
Relations of voltage and current density with circuit resistance, total amounts of O species transported and extracted, and promotion factors during 5 min CH_4 flow

Case	External circuit resistance (Ω)	Voltage (V)	Current density[a] (mA/cm^2)	O species transported[b] ($\mu mol/cm^2$)	Lattice O extracted[c] ($\mu mol/cm^2$)	Promotion factor, σ
A	1	0.13	43.5	67.6	72.1	1.07
B	6.2	0.61	23.5	36.6	42.3	1.16
C	52	0.77	15.9	24.6	31.8	1.29
D	6000	1.10	5.1	8.0	10.9	1.36
E	15000	1.21	1.1	1.7	2.6	1.5
Open circuit	–	1.22	0	0	1.3	–

[a] Average value of the measured current density during 5 min CH_4 flow. The area is in terms of the anode area.
[b] The amount of oxygen species transported from cathode TPB for the generation of the measured current.
[c] The amount of lattice oxygen species additionally extracted from anode-side bulk.

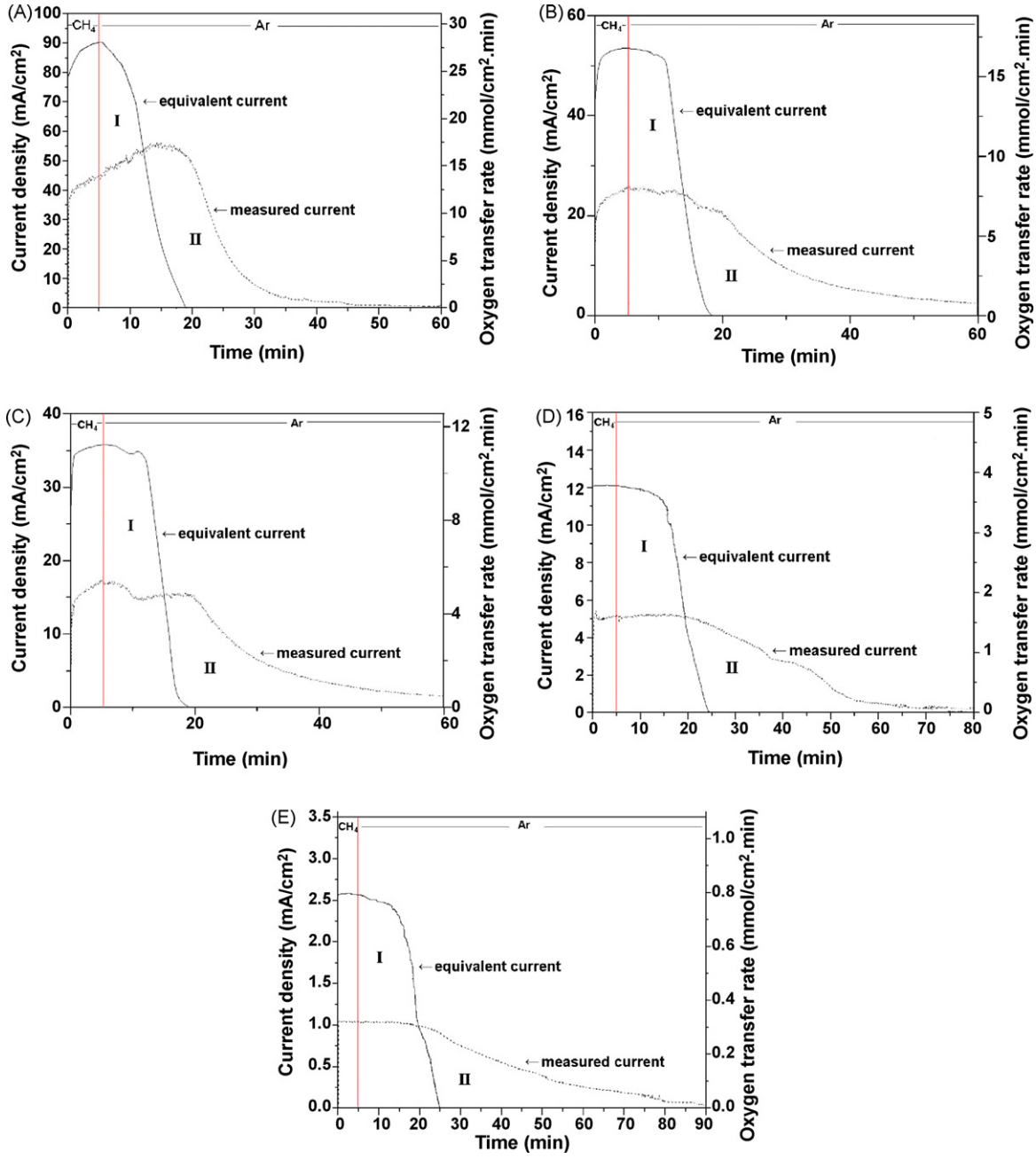

Fig. 3. Profiles of current densities vs. time. 5 min CH_4 flow. A–E as in Table 1. Zones I and II are defined as in Fig. 2.

The effect of electrochemical promotion on lattice-oxygen extraction from YSZ bulk observed in this work can be revealed by a promotion factor of lattice-oxygen extraction, σ, defined as

$$\sigma = \frac{\text{amount of lattice O extracted}}{\text{amount of O species transported}} \quad (2)$$

where the "lattice O extracted" denotes the total amount of the oxygen species additionally extracted from the anode-side bulk lattice, as indicated by the total area of zone I in Fig. 3, and the "O species transported" denotes the total amount of the oxygen species transported from cathode TPB to the anode TPB so as to generate the measured current. In other words, σ denotes the electrochemically promoted extraction of lattice oxygen per O species transported to generate the measured current. As shown in Table 1, σ increases as the voltage increases. Notably, the amount of O species transported is equivalent to the measured current and thus the electrochemical promotion of lattice-oxygen extraction from the support bulk indicates that the amount of the support-supplied lattice oxygen for the anode reaction is not limited by the electrical current.

Considering syngas generation for its conversion to methanol, partial oxidation of methane to form only CO without water formation should give the best result, with a product gas composition of $H_2/CO = 2$. However, some hydrogen may be adsorbed and oxidized to form H_2O. Nevertheless, Fig. 1

Table 2
Amounts of total CO_x formation during CH_4 plus argon flow and O_2 de-coking as well as O_2 de-coking time

Case[a]	CO_x formation[b] (μmol/cm^2)		O_2 de-coking time[e] (min)
	CH_4 plus Ar flow[c]	O_2 de-coking[d]	
A	331.6	0.34	28
B	161.8	1.05	103
C	109.3	3.11	389
D	59.7	6.54	670
E	11.7	13.7	850
Open circuit	1.13	1.11	524

[a] A–E as in Table 1.
[b] CO_x means both CO and CO_2. The area is in terms of the anode area.
[c] From the start of methane flow into argon flow until both CO and CO_2 formations become zero.
[d] Removal of the remaining coke with 100 ml/min of 20% O_2 in argon at 800 °C. Only CO_2 was detected.
[e] The time for O_2 de-coking till zero CO_2 formation.

shows that H_2O formation decreases and becomes zero with increased methane reaction. This is beneficial to syngas generation. Notably, increased extent of methane reaction can be associated with increased amount of deposited carbon, which reduces the area of the Ni surface for hydrogen adsorption. This is frequently considered as anode deactivation; however, the deposited carbon species can be the "fuel" to generate the electrical current as described above.

Table 2 reveals that, with decreasing current density from case A to case E, the amount of total CO_x formations during methane plus argon flow decreases but that during O_2 de-coking increases; moreover, the O_2 de-coking time also increases. This indicates that the SOFC ability to utilize the deposited carbon species from methane decomposition for the co-generation of electrical current and syngas decreases with decreasing current density. Notably, although the amount of CO_x formation during O_2 de-coking under open circuit is much smaller than that of case C, the O_2 de-coking time under open circuit is much longer. Notably, longer O_2 de-coking time means a more severe coking problem to the anode to deactivate it. Therefore, a high current flow can reduce the coking problem.

3.3. CO and CO_2 formations

Fig. 4 shows that the formation rate of CO is much higher than that of CO_2 for each case and there is a period of the formation of only CO but not CO_2. This is beneficial to syngas generation. From case E to case A, with the current density increasing, both CO and CO_2 formation rates increase. Nevertheless, the extent of the increase of the CO formation rate is higher than that of CO_2 and thus the CO selectivity increases. These are also revealed in Table 3. Moreover, Fig. 4 shows that the self de-coking periods in cases D and E become longer than those in cases A–C; this is in agreement with the results in Table 2 that much higher amount of deposited carbon was not self de-coked and need O_2 de-coking, and the O_2 de-coking time becomes much longer for cases D and E.

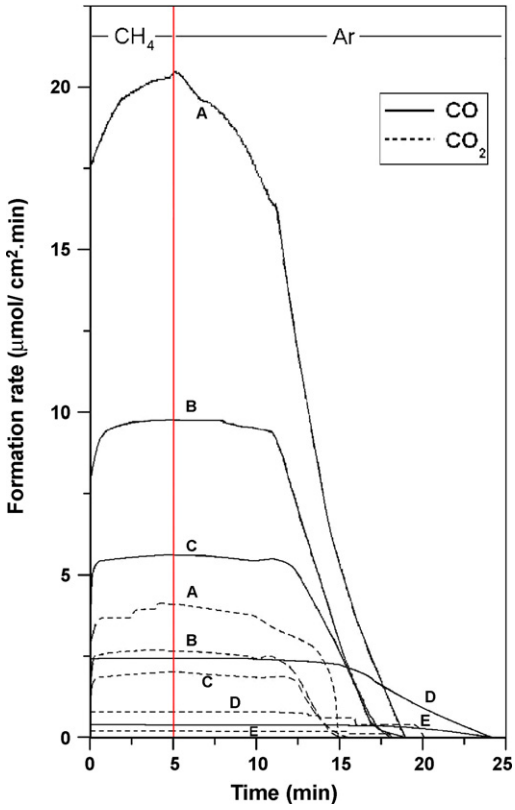

Fig. 4. Profiles of CO and CO_2 formation rates vs. time. 5 min CH_4 flow. A–E as in Table 1.

The rate enhancement ratio, ρ, for electrochemical promotion is defined as [10]

$$\rho = \frac{r}{r_0} \tag{3}$$

where r is the electrochemically promoted reaction rate and r_0 is the open-circuit reaction rate. Notably, this ratio can be considered as a dimensionless reaction rate as normalized in terms of the open-circuit reaction rate. Fig. 5 shows that both rate enhancement ratios of CO and CO_2 formations are inversely linearly related to the voltage. This is the well-known electrophilic behavior, that is, the effect of electrochemical promotion increases with decreasing potential [6].

Fig. 6 shows that the rate enhancement ratios of CO and CO_2 formations are linearly related to current density; the enhancement ratio increases with increasing current density.

Table 3
Total amounts of CO and CO_2 formations and CO selectivity during 5 min CH_4 flow

Case[a]	CO (μmol/cm^2)	CO_2 (μmol/cm^2)	CO selectivity[b]
A	92.8	22.7	0.803
B	49.6	13.9	0.781
C	34.7	10.3	0.771
D	11.1	3.59	0.756
E	2.05	1.05	0.661
Open circuit	0.73	0.30	0.71

[a] A–E as in Table 1.
[b] CO selectivity = amount of CO/(amount of CO + amount of CO_2).

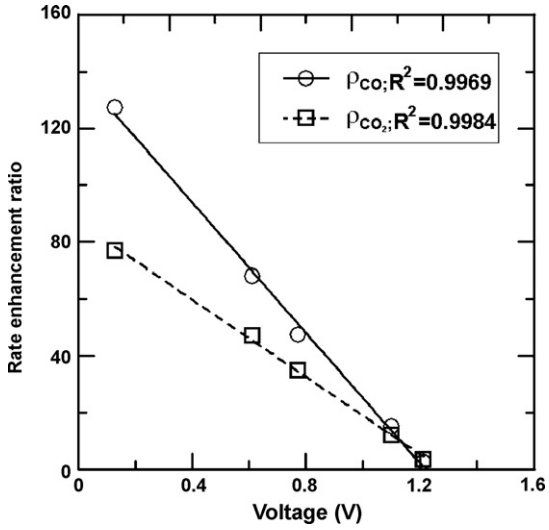

Fig. 5. Linear regression variations of the rate enhancement ratios of CO and CO_2 formations with voltage.

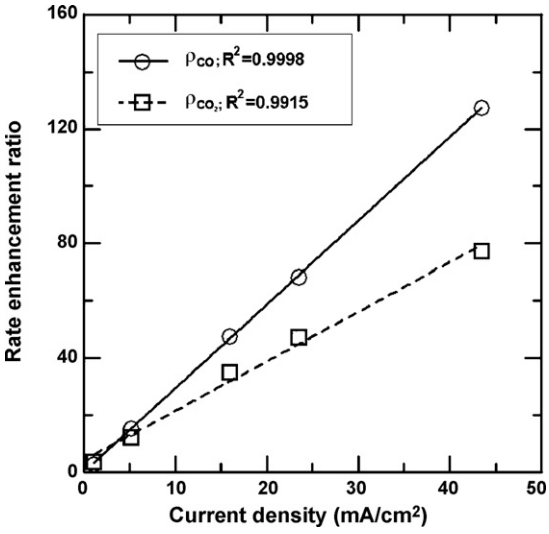

Fig. 6. Linear regression variations of the rate enhancement ratios of CO and CO_2 formations with current densities.

Nevertheless, the effect of electrochemical promotion of CO can be much higher than that of CO_2 at high current density. Moreover, Table 4 reveals that the formation rate of CO per O species supplied to the anode surface increases but that of CO_2 decreases with increasing current density, from cases E to A. This is beneficial to syngas generation. Notably, the amount of O species in Table 4 consists of those associated with the measured current and those extracted from the bulk lattice due to electrochemical promotion.

Table 4
Variations of electron charge, and CO and CO_2 formed, per oxygen transferred for anodic reaction during 5 min CH_4 flow

Case[a]	e^-/O[b]	CO/O	CO_2/O
A	0.967	0.664	0.163
B	0.928	0.628	0.177
C	0.873	0.614	0.183
D	0.843	0.589	0.190
E	0.790	0.478	0.244

[a] A–E as in Table 1.
[b] Average electron charge, number of electrons transferred from cathode TPB, per O species reacted at the anode surface.

Table 5
Results of regression analysis ($R = ax^n$) of average formation rate[a] (R) of CO and CO_2 vs. average oxygen transfer rate[b] (x)

Reaction	a	n
CO formation	0.502	1.08
CO_2 formation	0.239	0.886

[a] Calculated by dividing the total formation rate of CO and CO_2, respectively, during 5 min CH_4 flow by 5 min.
[b] Calculated by dividing the total oxygen transfer rate, i.e. O species transported plus lattice O extracted, during 5 min CH_4 flow by 5 min.

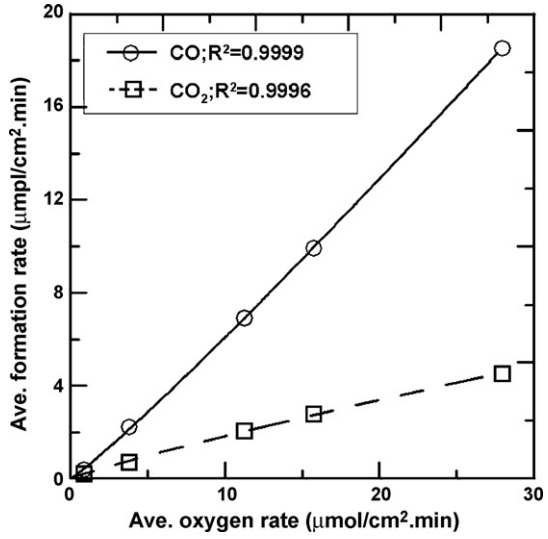

Fig. 7. Regression analysis ($R = ax^n$) of average formation rate (R) of CO and CO_2 vs. average oxygen transfer rate (x).

The average formation rate (R) of CO and CO_2 can be related to the average transfer rate (x) of the oxygen species, which consists of the oxygen species transported from the cathode TPB and the lattice oxygen species extracted from the anode-side bulk,

$$R = a\,x^n \tag{4}$$

Table 5 presents the constants a and n of Eq. (4) from a regression analysis, shown in Fig. 7. It is seen that the rate dependence of CO formation on the oxygen transfer rate, which is related to current density, is higher than that of CO_2 formation.

4. Discussion

4.1. Electrochemical promotion of bulk lattice-oxygen extraction

The electrochemically promoted reaction rate can be related to the applied potential, η, by an equation of the form [27],

$$\ln\left(\frac{r}{r_0}\right) = \frac{\alpha e \xi \eta}{kT} + \frac{\beta e}{kT} \tag{5}$$

where α and β are empirically determined constants, e is the charge of an electron, k is the Boltzmann constant, T is the operating temperature. Additionally, ξ is the relationship between the change in electron extraction potential, $\Delta\Phi$, and the applied potential,

$$\Delta\Phi = \xi\eta \quad (6)$$

Metcalfe [27] pointed out that ξ depends on the operating conditions and the electrode morphology.

In this work, the operating temperature is constant; thus, ln (r/r_0) can be plotted versus η to obtain the values of $\alpha e\xi/kT$, shown by the various slopes in Fig. 8. Notably, the applied potential (η) in Eq. (5) is equivalent to the generated potential (voltage) of the operating SOFC in this work. Thus, the variation of ξ is demonstrated, noting that $\alpha e/kT$ is a constant. This indicates that the variation of the external circuit resistance, shown in Table 1, can cause a variation in ξ. Fig. 8 reveals that the variation of ξ depends also on the reaction type, CO or CO_2 formation. This means that the electron extraction potential is not constant [27]. Since the extraction of the lattice oxygen species may involve electron, it may be proposed that the extraction potential of the lattice oxygen species is not constant. Therefore, the electrochemically promoted extraction of lattice oxygen may be influenced by both the operating condition and the reaction type, as confirmed by the above results.

The oxygen species for generating the measured current is from the cathode-side gas phase via dissociation and charge transfer, that is, $O_2 \leftrightarrows 2O$ and then $O + 2e^- \leftrightarrows O^{2-}$. The O^{2-} ion is usually considered to be the form of the oxygen species which can migrate in the bulk lattice of the oxygen-ion conducting materials. However, when close to the catalyst surface, the following scheme of oxygen reduction may be assumed: $O_2 \leftrightarrows O_2^- \leftrightarrows O_2^{2-} \leftrightarrows 2O^- \leftrightarrows 2O^{2-}$ [28]. The charged oxygen species which emerge at the three-phase boundary and spill over the electrode surface can be either O^- or O^{2-} [29]. Thus, when the O^{2-} ion is transported to the anode bulk, it may donate an electron to the anode-side lattice oxygen to form the $O^{\delta-}$ ion ($\delta = 1$ for this case). This is confirmed by the results as shown in Table 4, that is, the $O^{\delta-}$ species which are transferred in the anode-side bulk have δ values close to or less than one. Consequently, more oxygen species in the bulk phase of the oxygen-ion conducting materials become mobile and additional amount of the lattice oxygen species in the anode-side bulk can be extracted and transported to the anode surface for CO and CO_2 formations. Therefore, the anodic oxidation rate is promoted to become markedly higher than that by the oxygen species transported from the cathode TPB via the electrolyte. However, the oxygen species which carry less than two electrons may be considered to have lower mobility than those which carry two electrons. It may be proposed that the mobility of $O^{\delta-}$ species and thus the promotion effect of bulk lattice-oxygen extraction may be increased with increased potential; this is confirmed by Table 1, that is, the promotion factor (σ) increases with increased potential (voltage).

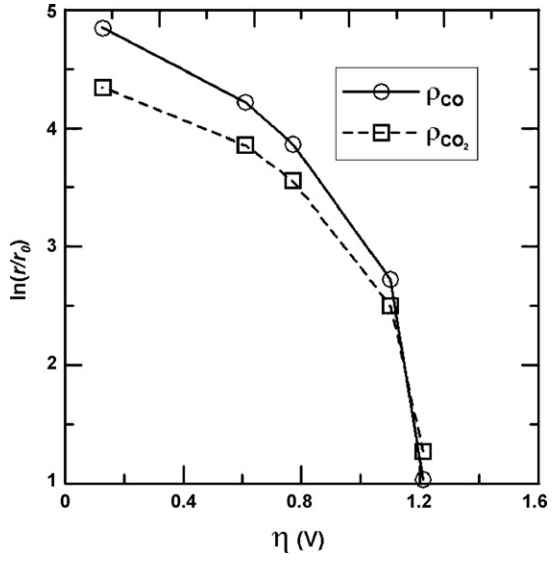

Fig. 8. Profiles of ln (r/r_0) vs. η (voltage) for CO and CO_2 formations. $\rho = r/r_0$.

According to the above hypothesis, the increase of the promotion factor of bulk lattice-oxygen extraction with voltage is due to the increased mobility of the $O^{\delta-}$ species with increased potential. Notably, the extraction of lattice oxygen from the anode-side bulk creates oxygen vacancy. In copper oxide, oxygen vacancy may be created via lattice oxygen reduction and migration when the lattice oxygen overcomes the energy barrier by a specific electrical field [30]. This is similar to the situation in this work, that is, the lattice oxygen receives an electron and the produced $O^{\delta-}$ ion migrates at increasing speed with increased potential. From a different point of view, the $O^{\delta-}$ species with smaller δ value needs higher potential to become mobile, as indicated by the results of Table 4 in association with Table 1. This may offer some explanation for the variation of ξ or the electron extraction potential with the operation condition. As shown in Table 1, a variation of the operation condition, i.e. an increase of the circuit resistance, results in an increase of the potential (voltage); this leads to a decrease of average electron charge per O species, shown in Table 4. Therefore, decreased number of electrons carried by the lattice oxygen is associated with higher potential for the O species to become mobile.

The occurrence of the fuel-free current is attributed to the deficiency of bulk lattice-oxygen concentration on the anode side after oxidation of the fuel, which extract additional amount of the lattice oxygen from the anode-side bulk without replenishment from the cathode TPB. Consequently, a deficiency of bulk lattice-oxygen concentration on the anode side is build up during fuel oxidation and thus, afterwards, the oxygen species migrate from the cathode TPB to the anode side to replenish the bulk lattice-oxygen concentration on the anode side to its initial state, which generates an electrical current. Therefore, the occurrence of the fuel-free current is a consequence of the electrochemically promoted extraction of bulk lattice-oxygen from the anode side. Notably, the process of oxygen replenishment starts right after a deficiency of the bulk lattice-oxygen concentration occurs and its rate increases with increased extent of the concentration deficiency; this is why zone II occurs before the exhaustion of the fuel, that is, before the equivalent current becomes zero, shown in Figs. 2 and 3.

4.2. Promotion of syngas generation

The above results indicate that higher CO and CO_2 formation rates, that is, higher methane conversion, lead to higher CO selectivity. Moreover, the electrochemically promoted extraction of bulk lattice oxygen results in higher CO selectivity. These are beneficial for syngas generation. With methane decomposition in the absence of gaseous oxygen, the formations of CO and CO_2 occur by oxidation with the oxygen species migrating from the support lattice to the metal surface via the metal-support interface [31]. Thus, electrochemical promotion of bulk lattice-oxygen extraction increases the supply rate of the oxygen species to the anode surface; consequently, the rates of CO and CO_2 formations are promoted. This promotion of the CO and CO_2 formation rates is partly due to the effect of electrocatalysis by electrical current and partly due to that of electrochemical promotion of bulk lattice-oxygen extraction. Table 1 reveals that the latter effect (lattice O extracted) is higher than the former one (O species transported); thus, the promotion factor (σ) is greater than one in all cases of this work. Nevertheless, although an increased potential (voltage) increases the promotion factor, lower potential and thus higher current density is needed for higher rate of syngas generation with higher CO selectivity. This is confirmed by Tables 1 and 3. On the other hand, with increased current density, although the promotion factor decreases, the absolute amount of the electrochemically promoted oxygen extraction increases, shown in Table 1. Therefore, electrochemical promotion of bulk lattice-oxygen extraction enhances the syngas generation.

Figs. 5 and 6 reveal that the effects of electrochemical promotion, i.e. the rate enhancement ratios, of CO and CO_2 formations are different. This may be attributed to that the dependences of CO and CO_2 formation rates on the oxygen transfer rate are different. Since the CO rate depends on the oxygen transfer rate at a higher extent than the CO_2 rate, revealed in Table 5, the promoted oxygen transfer rate by either the effect of electrocatalysis or that of electrochemical promotion should result in a higher rate of CO formation than that of CO_2 formation per oxygen species transferred, confirmed by Table 4.

Table 4 shows that higher oxygen transfer rate is beneficial to the formation of CO, but detrimental to that of CO_2. This is attributable to that CO_2 formation requires two O species in the neighborhood of the C species. If there is only one O species in the neighborhood of the C species, only CO can be formed. As the oxygen transfer rate increases, which means an increased mobility of the O species, the probability of only one O species in the neighborhood of the C species during its reaction time should increase; this probability increases as the reaction time becomes shorter. Notably, the oxygen transfer rate is directly related to the current density, shown in Figs. 2 and 3, and thus indicates the migration speed of the O species to the anode TPB. A higher current density means a higher migration speed of the O species and thus a shorter reaction time for the oxidation of the C species; consequently, CO formation is favored. Thus, it can be concluded that SOFC operation at high current density favors syngas generation.

Moreover, the above-observed phenomenon of higher CO selectivity associated with higher oxygen transfer rate, i.e. higher oxygen supply rate via the oxygen-ion conducting materials, is quite different from that associated with higher oxygen supply rate from the anode-side gas phase, which lowers the CO selectivity. Notably, only CO_2 is formed during O_2 de-coking in this work. Therefore, the phenomena associated with direct-methane SOFC, including electrochemical promotion of bulk lattice-oxygen extraction and fuel-free current as reported in this work, are worthy further investigation.

5. Conclusions

(1) A phenomenon of electrochemical promotion of lattice-oxygen extraction from the bulk phase of YSZ is observed. Markedly higher amount of oxygen than that equivalent to the measured current is extracted for anodic oxidation. This promotion effect increases as the potential (the generated voltage) increases.
(2) The electrochemically promoted extraction of bulk lattice oxygen is influenced by both the operating condition (the circuit resistance) and the reaction type (CO and CO_2 formations).
(3) A phenomenon of fuel-free current, i.e. the generation of electrical current without fuel either in the gas phase or at the surface, is observed. This is identified as a consequence of electrochemical promotion of lattice-oxygen extraction from the anode-side bulk.
(4) Both rate enhancement ratios of CO and CO_2 formations are inversely linearly related to the voltage.
(5) Both rate enhancement ratios of CO and CO_2 formations are linearly related to the current density.
(6) The dependence of CO formation rate on the oxygen transfer rate, which is related to the current density, is stronger than that of CO_2 formation rate.
(7) As the current density increases, both methane conversion and CO selectivity increase.
(8) Electrochemical promotion of bulk lattice-oxygen extraction enhances the syngas generation.
(9) SOFC operation at high current density favors syngas generation.

Acknowledgements

The National Science Council, Republic of China, is acknowledged for financial support under project number NSC 94-2214-E-007-001. The authors thank Mr. Ruei-Ming Huang for the assistance in the experimental work.

References

[1] C.G. Vayenas, S. Bebelis, S. Ladas, Dependence of catalytic rates on catalyst work function, Nature 343 (1990) 625–627.
[2] C.G. Vayenas, S. Bebelis, I.V. Yentekakis, H.G. Lintz, Non-Faradaic electrochemical modification of catalytic activity: a status report, Catal. Today 11 (1992) 303–442.

[3] T. Tagawa, K. Kuroyanagi, S. Goto, S. Assabumrungrat, P. Praserthdam, Selective oxidation of methane in an SOFC-type reactor: effect of applied potential, Chem. Eng. J. 93 (2003) 3–9.
[4] A. Kaloyannis, C.G. Vayenas, Non-Faradaic electrochemical modification of catalytic activity 12. Propylene oxidation on Pt, J. Catal. 182 (1999) 37–47.
[5] D. Tsiplakides, C.G. Vayenas, Temperature programmed desorption of oxygen from Ag films interfaced with Y_2O_3-doped ZrO_2, J. Catal. 185 (1999) 237–251.
[6] S. Bebelis, M. Makri, A. Buekenhoudt, J. Luyten, S. Brosda, P. Petrolekas, C. Pliangos, C.G. Vayenas, Electrochemical activation of catalytic reactions using anionic, cationic and mixed conductors, Solid State Ionics 129 (2000) 33–46.
[7] J. Nicole, D. Tsiplakides, C. Pliangos, X.E. Verykios, Ch. Comninellis, C.G. Vayenas, Electrochemical promotion and metal-support interactions, J. Catal. 204 (2001) 23–34.
[8] A. Katsaounis, Z. Nikopoulou, X.E. Verykios, C.G. Vayenas, Comparative isotope-aided investigation of electrochemical promotion and metal–support interactions 1. $^{18}O_2$ TPD of electropromoted Pt films deposited on YSZ and of dispersed Pt/YSZ catalysts, J. Catal. 222 (2004) 192.
[9] A. Katsaounis, Z. Nikopoulou, X.E. Verykios, C.G. Vayenas, Comparative isotope-aided investigation of electrochemical promotion and metal-support interactions 2. CO oxidation by $^{18}O_2$ on electropromoted Pt films deposited on YSZ and on nanodispersed Pt/YSZ catalysts, J. Catal. 226 (2004) 197–209.
[10] C.G. Vayenas, Thermodynamic analysis of the electrochemical promotion of catalysis, Solid State Ionics 168 (2004) 321–326.
[11] C. Kokkofitis, G. Karagiannakis, S. Zisekas, M. Stoukides, Catalytic study and electrochemical promotion of propane oxidation on Pt/YSZ, J. Catal. 234 (2005) 476–487.
[12] D. Tsiplakides, S. Balomenou, A. Katsaounis, D. Archonta, C. Koutsodontis, C.G. Vayenas, Electrochemical promotion of catalysis: mechanistic investigations and monolithic electropromoted reactors, Catal. Today 100 (2005) 133–144.
[13] S. Brosda, C.G. Vayenas, J. Wei, Rules of chemical promotion, Appl. Catal. B: Environ. 68 (2006) 109–124.
[14] C.G. Vayenas, S. Brosda, C. Pliangos, The double-layer approach to promotion, electrocatalysis, electrochemical promotion, and metal-support interactions, J. Catal. 216 (2003) 487–504.
[15] J.B. Wang, J.C. Jang, T.J. Huang, Study of Ni-samaria-doped ceria anode for direct oxidation of methane in solid oxide fuel cells, J. Power Sources 122 (2003) 122–131.
[16] Y. Lin, Z. Zhan, J. Liu, S.A. Barnett, Direct operation of solid oxide fuel cells with methane fuel, Solid State Ionics 176 (2005) 1827–1835.
[17] C. Mallon, K. Kendall, Sensitivity of nickel cermet anodes to reduction conditions, J. Power Sources 145 (2005) 154–160.
[18] J.B. Wang, Y.S. Wu, T.J. Huang, Effects of carbon deposition and decoking treatments on the activation of CH_4 and CO_2 in CO_2 reforming of CH_4 over Ni/yttria-doped ceria catalysts, Appl. Catal. A: Gen. 272 (2004) 289–298.
[19] M. Ihara, K. Matsuda, H. Sato, C. Yokoyama, Solid state fuel storage and utilization through reversible carbon deposition on an SOFC anode, Solid State Ionics 175 (2004) 51.
[20] T.J. Huang, M.C. Huang, Electrochemical promotion of bulk lattice-oxygen extraction for syngas generation over Ni-GDC anodes in direct-methane SOFCs, Chem. Eng. J. 135 (2008) 216–223.
[21] T.J. Huang, M.C. Huang, A new phenomenon of a fuel-free current during intermittent fuel flow over Ni-YSZ anode in direct methane SOFCs, J. Power Sources 168 (2007) 229–235.
[22] J.B. Wang, S.Z. Hsiao, T.J. Huang, Study of carbon dioxide reforming of methane over Ni/yttria-doped ceria and effect of thermal treatments of support on the activity behaviors, Appl. Catal. A: Gen. 246 (2003) 197–211.
[23] T.J. Huang, C.H. Wang, Factors in forming CO and CO_2 over cermet of Ni-gadolinia-doped ceria with relation to direct methane SOFCs, J. Power Sources 163 (2006) 309–315.
[24] T.J. Huang, C.H. Wang, Methane decomposition and self de-coking over gadolinia-doped ceria supported Ni catalysts, Chem. Eng. J. 132 (2007) 97–103.
[25] T.J. Huang, C.H. Wang, Roles of surface and bulk lattice oxygen in forming CO_2 and CO during methane reaction over gadolinia-doped ceria, Catal. Lett., in press.
[26] Q.Y. Yang, K.J. Maynard, A.D. Johnson, S.T. Ceyer, The structure and chemistry of CH_3 and CH radicals adsorbed on Ni(1 1 1), J. Chem. Phys. 102 (1995) 7734–7749.
[27] I.S. Metcalfe, Electrochemical promotion of catalysis: I: Thermodynamic considerations, J. Catal. 199 (2001) 247.
[28] J. Zhu, J.G. van Ommen, H.J.M. Bouwmeester, L. Lefferts, Activation of O_2 and CH_4 on yttrium-stabilized zirconia for the partial oxidation of methane to synthesis gas, J. Catal. 233 (2005) 434–441.
[29] J. Fleig, J. Jamnik, Work function changes of polarized electrodes on solid electrolytes, J. Electrochem. Soc. 152 (2005) E138.
[30] C.L. Chang, C.C. Hsu, T.J. Huang, Cathode performance and oxygen-ion transport mechanism of copper oxide for solid-oxide fuel cell, J. Solid State Electrochem. 7 (2003) 125.
[31] T.J. Huang, S.Y. Jhao, Ni-Cu/samaria-doped ceria catalysts for steam reforming of methane in the presence of carbon dioxide, Appl. Catal. A: Gen. 302 (2006) 325–332.